SindhUniv. Res. Jour. (Sci. Ser.) Vol. 53 (03) 257- 264 (2021)

SINDHUNIVERSITYRESEARCHJOURNAL(SCIENCE SERIES)

Investigation the fault in a Rotating Machineby Utilizing Vibration Technique

S. BHATTI[++], A. A. SHAIKH[++], A. MANSOOR*, W. A. SHAIKH**

Department of Basic Science and Related Studies, Mehran UET. Jamshoro

Received 13th January 2021and Revised 26thAugust 2021

Abstract: The maintenance of a machine before the faults will become increased the life of machinery component and also increased the operational reliability, reduced machinery down time, cost saving, second failure etc.In this study analysis the fault in a machine at early stage to enhance the life of machine .The experimental setup is design to generate real time data of three different bearings whose rotational speed is decreased gradually (i) perfectly healthy bearing (ii) inner fault bearing (iii) outer fault bearing respectively. The readings of the datasets in the time-domain frequency for a duration of 10 seconds.. Further analysis the behavior of the datasets by using statistical & mathematical techniques such as Kurtosis, Spectrum Kurtosis and Kurtogram are used for high amplitude of the waveform and mathematical technique Fourier Transformation apply to convert the time signal data into frequency domain and then analysis the harmonics of the frequency at BPFI (Ball Pass Frequency Inner)and BPFO (Ball Pass Frequency Inner)conditions to detect the inner race fault and outer race fault in the bearing.

Keywords: Kurtosis, Spectral Kurtosis, Kurtogram, Fourier Transform (FT), Power Spectrum, Envelope Spectrum

1. INTRODUCTION

Ultimate objective of any maintenance methodology is to maximize operational availability of machinery with minimum down time and low running and maintenance cost. Nevertheless, despite not compromising on quality and reliability, inherent problems of repair/ maintenance have always remained a challenge for the maintenance world. The maintenance of a machine before the faults will become increased the life time of machinery component and also increased the operational reliability, reduced machinery down time, cost saving, second failure etc. Various methods have been developed for machine fault diagnosis and condition monitoring, such as vibration monitoring, temperature monitoring, chemical analysis, acoustic emission monitoring, sound pressure monitoring, and laser monitoring (Zhou, *et al.*, 2007). To detect the fault in a machine by using vibration analysis method many methods are used in literature such as in the statistically method to measure the noise(fault) RMS, kurtosis, skewness, Crest Factors, Peak-value, Visual, particle count, spectrograph etc. The mathematical process convert the time domain into frequency domain understand the behavior of the signal by using FT and then, FFT, and Wavelet Transform Hilbert-Huang Transformation, etc.

2. LITERATURE REVIEW

To detect fault in the machine various methods were used in literature the most common technique is numerous traditional FIs techniques for rotating machinery, in FI the RMS is the greatest common technique applied to predict the RUL of machinery (Zhu, *et al.*, 2014) (Večeř, *et al.*, 2005) Predict the RUL of rolling elements of bearing by used kurtosis and RMS Techniques (Li, *et al.*, 2015) (Huang, *et al.*,2017). also used RMS technique to forecast the RUL of bearings (Huang, *et al.*,2017) (Huang, *et al.*,2015). RUL of bearing was forecast by take out the RMS and coefficient of wavelet transform used to obtain the crest values (Malhi, *et al.*, 2011). Furthermore, vibrating signals frequency were used to brain the FIs. Predict the RUL of gears by takeout the power density of the gear-mesh frequency from the domain. (Gašperin, *et al.*, 2011) estimated the mean of the faulty frequency ad its harmonics as a FI of push bearings. In signal processing to analysis the time domain data, new FIs techniques were developed by researchers by using statistical characteristics. Applied the correlation coefficient technique concerning dual series of vibrating signals (Medjaher, *et al.*, 2013). Some new FIs were also established from the entropy of time-domain signals. Some investigators used the frequency domain of signals to take out the new FIs (Li, *et al.*, 2017) (An, *et al.*, 2016). the FIs of bearing is obtained by vibration analysis of a signal. Précised the estimating the spectral flatness (Qian, *et al.*, 2014). (Soualhi *et al.*, 2017). Used Hilbert-Huang Transformation to investigated vibration signals and obtained FIs from extracted damaged frequencies (Soualhi, *et al.*, 2017).

[++]Corresponding E-mail: saima.bhatti@faculty.muet.edu.pk, asif.shaikh@faculty.muet.edu.pk
*National University of Sciences and Technology (NUST), PNEC campus Karachi kp.ude.tsun.cenp@rartsiger
**Department of Mathematics & Statistics, QUEST. Nawabshah: wajid@quest.edu.pk

3. (MATERIAL AND METHODS

In this present work the testing rig that has been used for the generation of bearing data is SpectraQuest® machinery which is widely used for study faults and defects. The MFS-PK5M is specifically designed to generate vibrant data for the development of new algorithms, techniques and understanding regarding the concept. It excellently emulates the phenomena of practical machinery. A Pictorial view is given below representing the testing apparatus. **(Fig. 1).**

Fig 1:- Experimental Setup

The data is gathered by the accelerometer placed on the end of the experimental bearing. The accelerometer is placed on the housing of the bearing for the collection of vibrant data. The model number of the accelerometer used is ICP Accelerometer, Model 623C01. Datasheet of the respective model would be attached at the end of the dissertation for further references and information. The transmission of the data from the accelerometer to the data-logging setup is done using the NI(National Instruments) acquisition boards (Model No. USB 6212 BNC). Along with all the sensors mentioned above rotary encoders of the model number EPC 775 are also placed on the shaft.

4. RESULTS AND DISCUSSION

Case I: The first step is note down the reading of a healthy bearing whose rotational speed is being decreased gradually in time domain signal showing in **(Fig.2)** which shows that the amplitude of the waveform is gradually being reduced.

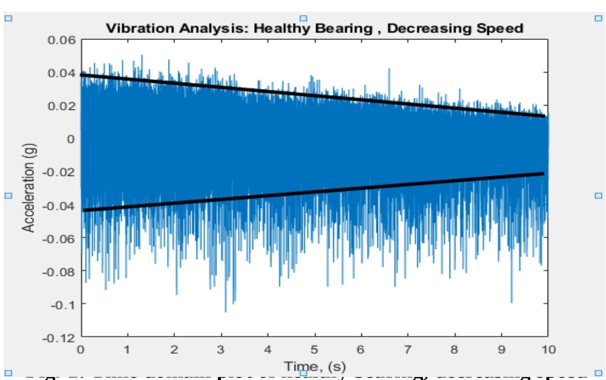

It is also notice that the rotational speed of the drive is being reducedfrom28.9Hz to 13.7Hz.Further we can verify the results using the Eq(1)

$$\frac{\textbf{RotationalSpeedattheend}}{\textbf{RotationalSpeedattheStart}} = \frac{13.7}{28.9} = 0.47 \qquad \text{Eq (1)}$$

The zoomed-in view details that the waveform is regular with very few spikes or impulses. This is one of the first steps in deducing that the dataset belongs to a healthy bearing.**(Fig. 3)**

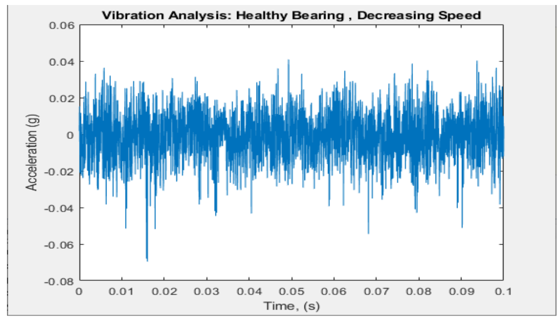

Fig 3:Zoomed-in view of healthy bearing decreasing speed

The next step in the process to convert time domain signal into frequency domain by Using the power spectrum method, the FT is used to make sure that the signal is plotted in the frequency domain show in **(Fig.4).**

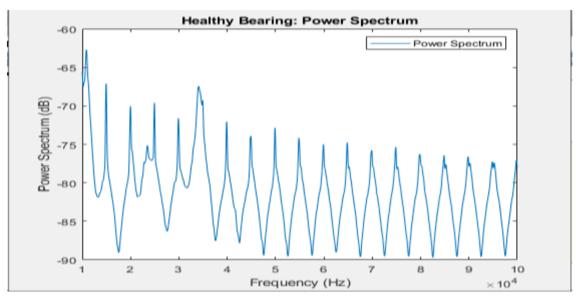

Fig.4: Fourier transform of healthy bearing, decreasing speed

The FT result is regular with no irregular frequency pulse at the BPFI(Ball Pass Frequency Inner) or BPFO(Ball Pass Frequency Outer).As a technique of cross-validation , the actual fourier equation has been calculated using mathematical derivation to check if it fits correctly on the acquired graph or not. The calculated Fourier equation is presented below:

$$\boldsymbol{f(x) = -81.38 + 4.802Cos(x) + 0.7669Sin(x)Eq(2)}$$

To check if the **Eq(2)** is correctly calculated or derived, we super impose the **Eq(2)** on the graph**(Fig.4)** from the acquired dataset to verify their compatibility.

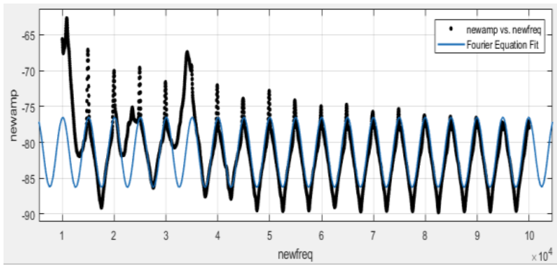

Fig 5: Fourier Equation fit on Fourier transform of healthy bearing, decreasing speed

As it is evident from the **(Fig. 5)** that both the graphs are very much compatible and almost fit perfectly on top of each other, proving that the equation is calculated correctly.

The next step in the vibration analysis process is to perform the envelope spectrum analysis. The envelope spectrum analysis makes sure that all the unwanted or undesired signals are removed and only the original signal is viewed to check for any irregularity or defects. The following image displays the result of the envelope spectrum analysis

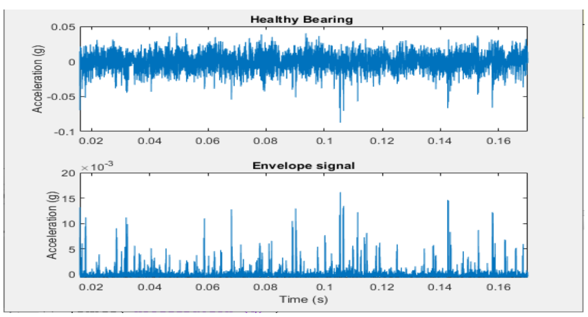

Fig 6: Envelope spectrum results

(Fig: 6) is divided into two portions the upper portion consists of the normal signal acquired from the healthy bearing. The lower portion represents the resulting waveform after the envelope spectrum analysis. This shows how much noise or unwanted signals are present in the original signal.

A zoomed-in view of the envelope signal will provide us with a better understanding of the waveform given as:

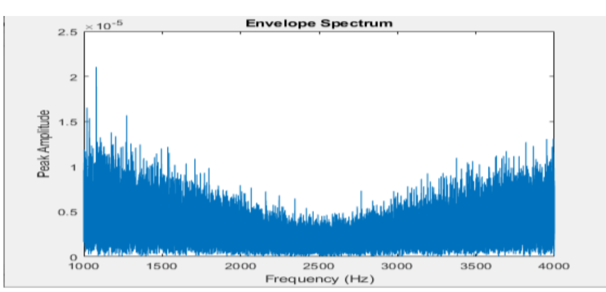

Fig 7- zoomed in view to check harmonics

(Fig:7) shows that no irregular peaks or impulses are present at either BPFI(Ball Pass Frequency Inner) or BPFO(Ball Pass Frequency Outer) which is an indication that no fault or defect is present in the bearing and the bearing is in fact a healthy one.

Case II: The first step in the vibration process is to load the dataset values of the inner race with decreasing rotational speed is showing time-domain graph as below:

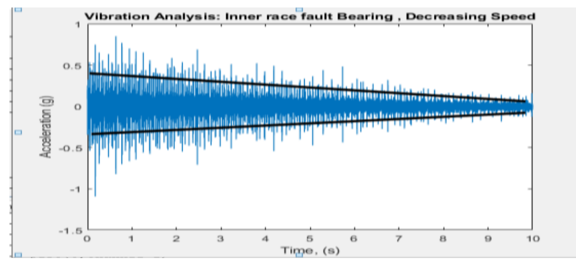

Fig 8- Time domain plot of an inner race faulty bearing, decreasing speed

The first aspect of the dataset parameter is being verified explicitly as it is evident that the amplitude of the waveform is experiencing a reduction in the amplitude. This reduction is although not proportional to the one being done on the rotational speed. The same formulae used in the above segments are applied in this to check for if the amplitude variations are in proportion or not:

$$\boldsymbol{Fromthegraph} = \frac{\mathbf{0.02}}{\mathbf{0.4}} = \mathbf{0.05} \qquad \textit{Eq(3)}$$

$$\boldsymbol{Theoreticalvalue} = \frac{\mathbf{9.9}}{\mathbf{24.3}} = \mathbf{0.41} \qquad \textit{Eq(4)}$$

$$\boldsymbol{error} = \frac{\mathbf{0.05-0.41}}{\mathbf{0.41}} \boldsymbol{X}\mathbf{100} = \mathbf{90\%} \qquad \textit{Eq(5)}$$

As observed from the formulae above, it is clear that the difference between the theoretical and actual value is considerable and could not be neglected. The zoomed-in view of time domain signal shown in **(Fig.9)**

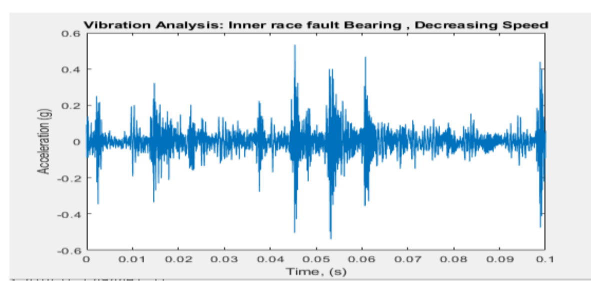

Fig 9- Zoomed-in view of an inner race faulty bearing, decreasing speed

(Fig.9) shows that the level of impulsiveness or peakedness in the time-domain waveform of the following dataset is very high from the mean value of the waveform. It is high as compared tothe healthy bearings and this could also be verified visually.

The next step in the process of vibration analysis would be to change the orientation of the waveform. The waveform is presently in the time-domain perspective, and to check for any unwanted frequencies in the system which might have crept in due to defects in the bearing. The Fourier transform is therefore computed and plotted to check for perturbations in the system. The Fourier transform is applied using the power spectrum analysis for a better pictorial view of the results. **(Fig. 10)**

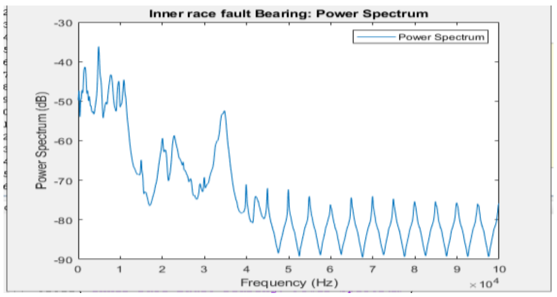

Fig. 10-Fourier Transform of inner race faulty bearing, decreasing speed

By studying this graph, a conclusion can be made that the bearing dataset system does have some unwanted frequencies which might be an indication of a potential fault or defect.

The next step in the process is to calculate the Fourier equation using the data mathematically and check what information the equation provides us about the data. If the equation contains more number of terms than it would indicate the presence of multiple harmonics and forces acting on the bearing which would signal that the bearing is not running smoothly. The equation of the Fourier transform is given below:

$$f(x) = -61.97 + 30.77Cos(xw) \\ -4.174Sin(xw) + 13.74Cos(2xw) \\ -15.22Sin(2xw) - 3.547\,cos(3xw) \\ -18.33Sin(3xw) - 5.213Cos(4xw) \\ -10.57Sin(4xw) - 10.8Cos(5xw) \\ -3.325Sin(5xw) - 8.77Cos(6xw) \\ +1.203Sin(6xw) - 4.521Cos(7xw) \\ +4.292\,sin(7xw) - 2.465Cos(8xw) \\ +3.621Sin(8xw) \quad Eq(6)$$

As evident in the Eq(6), the number of terms are more and could have been even more if the calculation or obvious limitations would not have arisen. This is not like an equation of healthy bearing which involved only two components. As it contains many terms, it means that many harmonics (and even more) are contributing in the waveform which would mean that the bearing is indeed faulty. A next step could be to plot the Eq(6) on the acquired dataset waveform (Fourier transform). The result is given below:

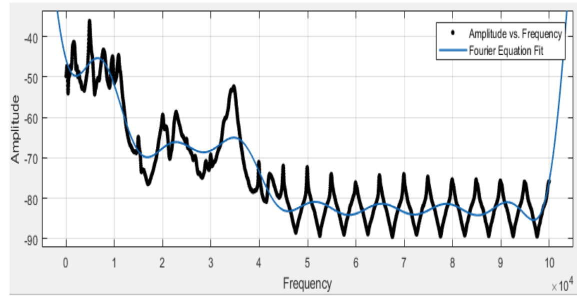

Fig 11- Fourier Equation fit on the Fourier transform

(Fig. 11) is an excellent example of showing that even though the equation contains a plethora of harmonics, it still does not fit properly signaling the presence of many other harmonics. These harmonics are a very basic indicator of a fault in the bearing.

The next step in the process is to carry out the envelope spectrum analysis that allows the seclusion of the original signal from the unwanted noise signals. The result of the envelope spectrum analysis is given in **(Fig. 12)**

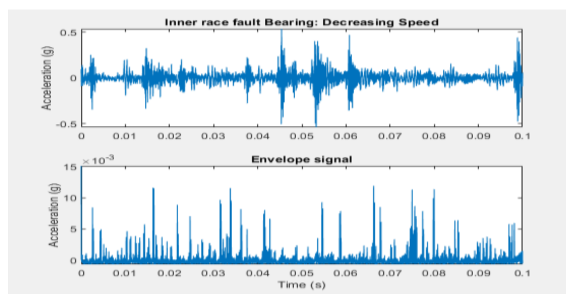

Fig.12- Envelope spectrum results

The signal after undergoing the envelope spectrum process should be looked at in a zoomed-in view with the domain changed from time-domain to frequency domain to check for any frequency on the BPFO (Ball Pass Frequency Outer) and BPFI(Ball Pass Frequency Inner). Any peak or impulse at these frequencies would mean that as the bearing rotates , at these particular points of either the inner race or the outer race, it is experiencing a perturbation or disturbance indicative of a fault in that particular part of the bearing.

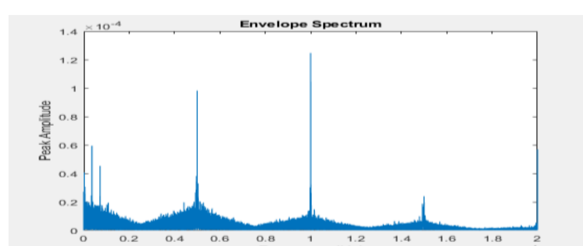

Fig 13- Zoomed-in view to check harmonics

(Fig. 13) shows the result of the zoomed-in view and it is evident in the image that the bearing is suffering from a disturbance at the BPFI(Ball Pass Frequency Inner) → 500Hz. This alone can help us in deciding and identifying that the fault in the bearing is located at the inner race.

Another cross check to the identification of a fault in the inner race could be finding the kurtosis value of the dataset. As mentioned in the previous section, it was concluded that any bearing with an inner race fault would have a greater kurtosis value as compared to the healthy bearing. The kurtosis value graph is given in the image below:

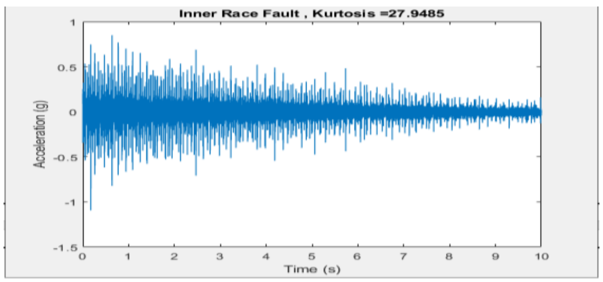

Fig 14- Kurtosis value graph

As shown in the graph above that the kurtosis value is about 28 which is more than the one obtained in the healthy bearing datasets(all). This is a major indicator of a fault in the inner race of the bearing as whenever a bearing will complete its one rotation and the part that is suffering a fault registers an abnormal reading in the accelerometer, it causes a spike in the waveform resulting in an unusual Fourier transform and eventually graph.

Case III: The process of vibration analysis in this segment is a little different as the bearing is experiencing a decrease in the rotational speed and the bearing infect does contain a fault in the outer race. The time domain plot of the vibration signal is shown below:

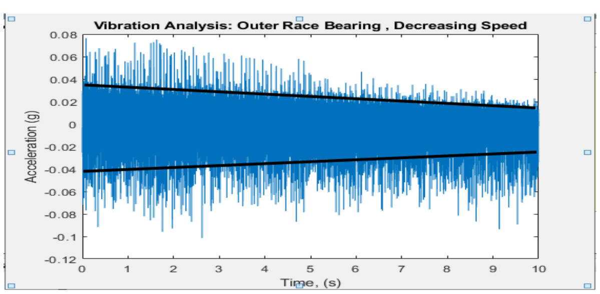

Fig. 15-Time domain plot of outer race faulty bearing, decreasing speed

As it can be seen in **(Fig.15)** the bearing is in fact experiencing a decrease in its amplitude as it should be with a decrease in the rotational speed. To verify if the decrease in amplitude is proportional to the decrease in rotational speed, the following formulae is used:

$$\boldsymbol{Fromthegraph} = \frac{\mathbf{0.016}}{\mathbf{0.043}} = \mathbf{0.37} \boldsymbol{Eq}(\mathbf{7})$$

$$\boldsymbol{Theoreticalvalue} = \frac{\mathbf{9.8}}{\mathbf{24.9}} = \mathbf{0.39} \boldsymbol{Eq(8)}$$

$$\boldsymbol{Error} = \frac{\mathbf{0.39-0.37}}{\mathbf{0.39}} \boldsymbol{X}\mathbf{100} = \mathbf{5\%} \qquad \boldsymbol{Eq(9)}$$

The results from the above calculation show that the amplitude is decreasing in proportion to the decrease in rotational speed. This makes the fault finding even difficult as the signal does not have any impulsiveness explicitly but implicitly. A better understanding of the signal could be achieved by having a look at the zoomed-in view of it shown below:

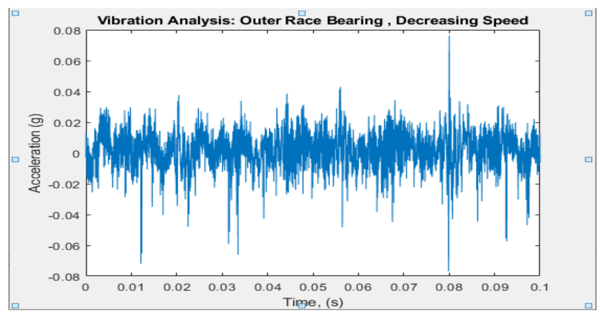

Fig.16-Zoomed-in view of outer race faulty bearing, decreasing speed

As it can be seen in the zoomed-in view, the signal is highly regular with very few peaks and oscillates with a fixed amplitude. The time-domain analysis is not doing any help in identifying the fault of the bearing.

To solve this problem, a different perspective or context of the signal is needed which would allow us to observe other traits about the signal. The other perspective is of the frequency domain which is achieved by computing the FT of the signal.

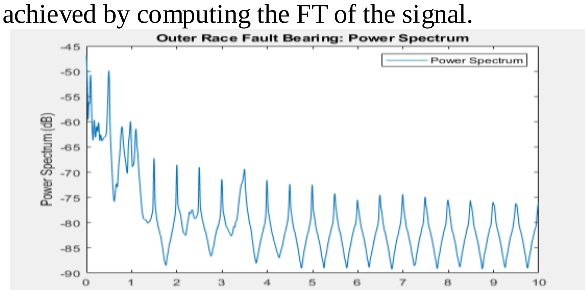

Fig 17-Fourier Transform of outer race faulty bearing, decreasing speed

The FT of the signal shows a disturbance in the initial portion in the **(Fig. 17).** This is the reason that the

FT is computed to identify any unwanted harmonics or impulses in the given signal. The FT equation is computed using calculation to check if the equation verifies the results presented by the above image. The Fourier equation is given in the following lines:

$$\begin{aligned} \boldsymbol{f(x) =} & \boldsymbol{-77.54 + 8.696Cos(xw)} \\ & \boldsymbol{+0.1802Sin(xw) + 5.664Cos(2xw)} \\ & \boldsymbol{-1.118Sin(2xw) + 3.711\,cos(3xw)} \\ & \boldsymbol{-1.609Sin(3xw) + 1.834Cos(4xw)} \\ & \boldsymbol{-0.5969Sin(4xw)} \textit{Eq(10)} \end{aligned}$$

By witnessing the **Eq. (10)**, it is evident that the signal does contain unwanted terms or harmonics but these are not nearly as much as in the case of an inner race faulty bearing. This fourier transform is a major distinguishing factor between a bearing with an inner race or outer race fault.

The **Eq. (10)** is plotted on the same fourier transform in **(Fig.18)** to observe how close the fit is. The resulting image is given below:

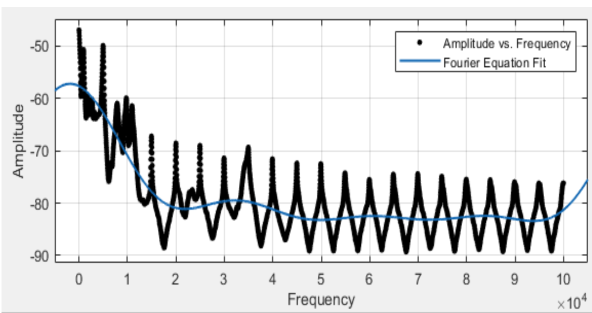

Fig. 18- Fourier Equation fit on Fourier Transform

The image above of the superimposing of both the graph proves that although the equation is derived up to four terms it still contains a considerable number of more harmonics that would have to be put in the equation for a better fit on the actual transform.

The next step is to carry out the envelope spectrum analysis of the original signal. The envelope spectrum analysis, as mentioned in all the cases above, removes any unwanted frequencies or signals from the original signal to provide us with an unadulterated signal.

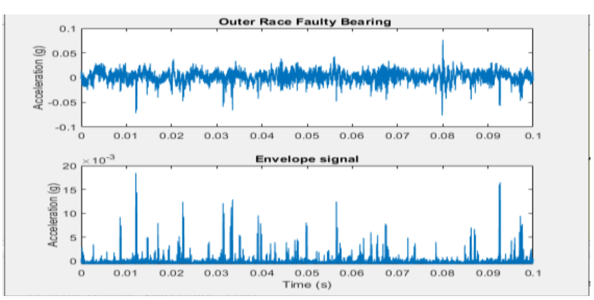

Fig19-Envelope spectrum results

The result of the envelope spectrum process is showing in **(Fig.19)** The envelope spectrum analysis as enabled the unwanted noise to be cancelled out which could be seen from the reduction of the noise floor in the signal. The other aspect that could be noticed is the fact that the signal peak has diminished to a much lower value.

The fourier transform of the envelope signal is then computed to better allow us to have a better look at the harmonics on the BPFO(Ball Pass Frequency Outer). This frequency is basically the fault frequency and any impulse or peak on these frequencies is an indication of a certain fault. The peaks presented in **(Fig. 20)** are located at the BPFO frequencies which makes us decide that the bearing is not running smoothly and is in fact experiencing a defect.

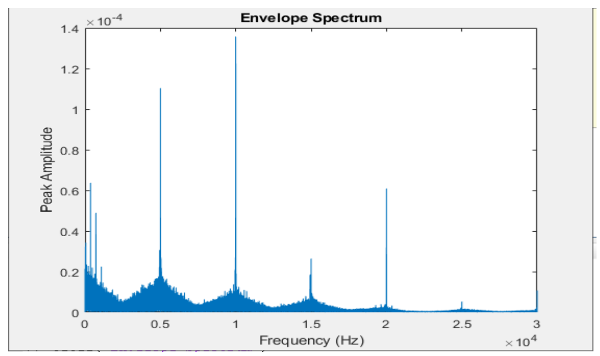

Fig 20-Zoomed-in view to check harmonics

To further add substance to our claim of it being a fault at the outer race, a few other techniques involving the kurtogram and kurtosis are performed. As we know from our experience in the previous cases that the kurtosis value of a bearing with an outer race fault lies right in between the kurtosis value of a healthy bearing and an inner race faulty bearing.

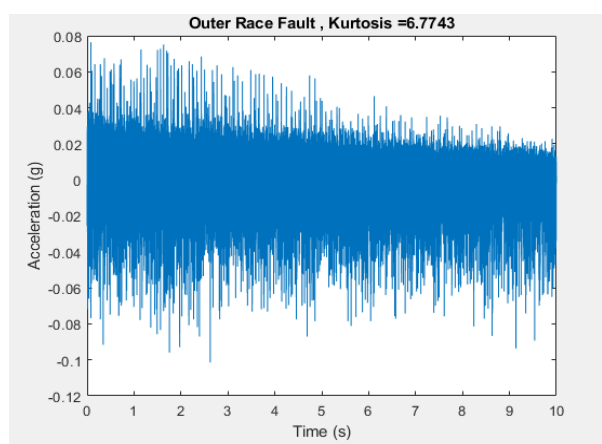

Fig.21- kurtosis value graph of outer race faulty bearing, decreasing speed

(Fig.21) shows that kurtosis value is known to be 6.8 which makes it more impulsive than a healthy bearing.

The next step in the process is to plot the kurtogram. The kurtogram is a technique that enables us to find the central frequency and the bandwidth of the signal. These parameters enable us to carry out the spectral kurtosis of the signal which using the 95% confidence interval method identifies unwanted peaks on the BPFO.The result of the kurtogram is shown in **(Fig.22)**

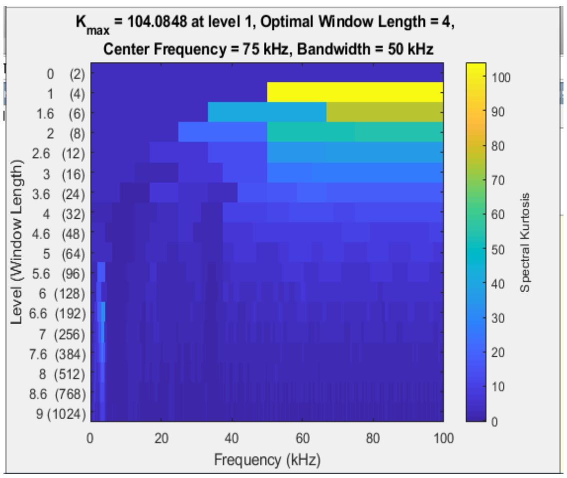

Fig. 22- Kurtogram of outer race faulty bearing, decreasing speed

The kurtogram identifies the central frequency to be at the 75 kHz mark and the bandwidth of the signal to be50kHz. This enables us to plot the spectral kurtosis Shown in **(Fig.23)**.

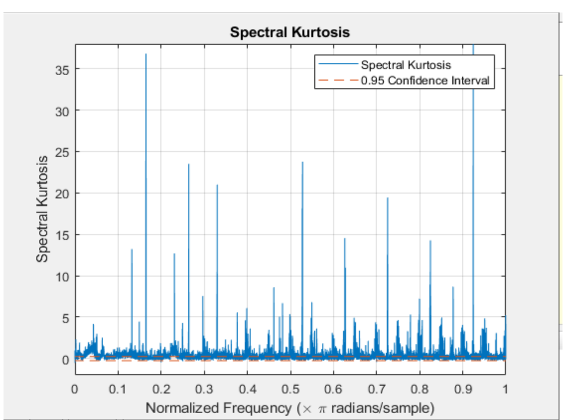

Fig 23-Spectral kurtosis of outer race faulty bearing, decreasing speed

The spectral kurtosis shows that the peaks are way out of the 95% confidence interval method proving us that the bearing does have a fault in the outer race.

5. CONCLUSION

This study conclude that the amplitude of a healthy bearing is regular with very few spikes or impulses and the rotational speed is reduce gradually from 28.9Hz to 13.7Hz. The envelope spectrum and the Fourier transform results indicate that the waveform is regular with no irregular frequency. In the second case the amplitude is not proportional to the rational speed and the kurtosis value is approximately 28 shows that the peakedness of the waveform is very high which indicate a fault in a bearing. The mathematically results of the FT and envelope spectrum shows that the bearing is running not smoothly it has multiple harmonics and bearing is suffering from a disturbance at the BPFI (Ball Pass Frequency Inner) → 500Hz this can help us in deciding and identifying that the fault in the bearing is located at the inner race. In case III the mathematically analysis that harmonics on the BPFO (Ball Pass Frequency Outer) is an indication of a certain fault. The amplitude of time domain is highly regular and have very few peaks. The result of Kurtosis value is 28 that shows fault in the bearing. The kurtosis value of a bearing with an outer race fault lies right in between the kurtosis value of a healthy bearing and an inner race faulty bearing. The kurtogram identifies the central frequency to be at the 75 kHz mark and the bandwidth of the signal to be 50 kHz. The statistical results shows that 95% confidence interval that the bearing does have a fault in the outer race.

REFERENCES:

An, D., N. H. Kim, and J. Choi, (2016) “Bearing Prognostics Method Based on Entropy Decrease at Specific Frequency,” in *18th AIAA Non-Deterministic Approaches Conference*.

Gašperin, M., Đ. Juričić, P. Boškoski, and J. Vižintin, (2011) “Model-based prognostics of gear health using stochastic dynamical models,” *Mech. Syst. Signal Process.*, vol. 25, no. 2, 537–548.

Huang,Z., Z. Xu, X. Ke, W. Wang, and Y. Sun, (2017) “Remaining useful life prediction for an adaptive skew-Wiener process model,” *Mech. Syst. Signal Process.*, vol. 87, 294–306,.

Huang, Z., Z. Xu, W. Wang, and Y. Sun,(2015) “Remaining useful life prediction for a nonlinear heterogeneous wiener process model with an adaptive drift,” *IEEE Trans. Reliab.*, vol. 64, no. 2, 687–700.

Li, N., Y. Lei, J. Lin, and S. X. Ding, (2015) “An Improved Exponential Model for Predicting Remaining Useful Life of Rolling Element Bearings,” *IEEE Trans. Ind. Electron.*, vol. 62, no. 12Pp.

Lei, Y., N. Li, and J. Lin, (2016) “A New Method Based on Stochastic Process Models for Machine Remaining Useful Life Prediction,” *IEEE Trans. Instrum. Meas.*, vol. 65, no. 12, 2671–2684,.

Li, H., Y. Wang, B. Wang, J. Sun, and Y. Li, (2017) “The application of a general mathematical morphological particle as a novel indicator for the performance degradation assessment of a bearing,” *Mech. Syst. Signal Process.*, vol. 82, 490–502.

Lin, D., M. Wiseman, D. Banjevic, and A. K. S. Jardine, (2004) “An approach to signal processing and condition-based maintenance for gearboxes subject to tooth failure,” *Mech. Syst. Signal Process.*, vol. 18, no. 5, 993–1007,

Loutas,T. H., D. Roulias, and G. Georgoulas, (2013) “Remaining useful life estimation in rolling bearings utilizing data-driven probabilistic E-support vectors regression,” *IEEE Trans. Reliab.*, vol. 62, 4, 821–832.

Malhi,A., R. Yan, and R. X. Gao, (2011) “Prognosis of defect propagation based on recurrent neural networks,” *IEEE Trans. Instrum. Meas.*, vol. 60, no. 3, 703–711.

Medjaher, K., N. Zerhouni, and J. Baklouti, (2013) “Data-driven prognostics based health indicator construction: Application to PRONOSTIA’s data,” in *Control Conference (ECC), European*, 1451–1456.

Qian,Y., R. Yan, and S. Hu, (2014). “Bearing degradation evaluation using recurrence quantification analysis and kalman filter,” *IEEE Trans. Instrum. Meas.*, vol. 63, no. 11, 2599–2610,

Večeř, P., M. Kreidl, and R. Šmíd, (2005) “Condition Indicators for Gearbox Condition Monitoring Systems,” *Acta Polytech.*, vol. 45, no. 6, 35–43.

Zhou, W., T. G. Habetler, and R. G. Harley, (2007) “Bearing condition monitoring methods for electric machines: a general review,” in *Proceedings of the IEEE International Symposium on Diagnostics for Electric Machines, Power Electronics and Drives (SDEMPED’07)*, 3–6.

Zhu, J., T. Nostrand, C. Spiegel, and B. Morton, (2014) “Survey of Condition Indicators for Condition Monitoring Systems,” *Annu. Conf. Progn. Heal. Manag. Soc.*, vol. 5, 1–13.